Rearrangement of the 1-oxaspiro[4.5]deca-6,9-dien-8-ylium ion. Part 1. A semiempirical (AM1), density functional and *ab initio* molecular orbital computational study †

Cedric W. McCleland,*[a] Giuseppe D. Ruggiero[b] and Ian H. Williams[b]

[a] *Department of Chemistry, University of Port Elizabeth, PO Box 1600, Port Elizabeth 6000, South Africa. E-mail: chacwm@upe.ac.za*
[b] *Department of Chemistry, University of Bath, Bath, UK BA2 7AY*

Received (in Cambridge, UK) 27th June 2001, Accepted 12th November 2001
First published as an Advance Article on the web 7th January 2002

The energetics of the ring-expanding rearrangement of the 1-oxaspiro[4.5]deca-6,9-dien-8-ylium ion **14** involving a 1,2-shift of either carbon or oxygen have been investigated through molecular orbital calculations at the semiempirical (AM1), *ab initio* (HF/z, HF/6-31G* and MP2/6-31G*) and density functional (B3LYP/6-31G*) levels of approximation. Our results have shown that rearrangement *via* migration by carbon is thermodynamically (and probably also kinetically) favoured over the alternative 1,2-shift by oxygen. The geometries and charge distributions computed for the structure **14** as well as the rearranged cations and possible transition structures are also described.

Introduction

We are currently investigating 1,5- *vs.* 1,6-cyclisation selectivities which pertain when γ-arylalkanols such as 3-arylpropan-1-ols and aryloxyethanols undergo ring-closure *via* their associated alkoxyl radical and aryl radical cation intermediates.[1–6] A range of alkoxyl radicals **1** have been generated previously in our laboratories through either photolysis of the appropriate γ-arylalkyl hypoiodites[1–3] or one-electron reduction of γ-arylalkyl hydroperoxides,[4–6] and aryl radical cations **2** through one-electron oxidation of the corresponding arylalkanols with $SO_4^{-\bullet}$.[4,5] While 1,6-cyclisation of these intermediates generally leads directly to six-membered ring products, discrete 1,5-cyclised products have been observed only in the hypoiodite reactions, in the form of spirocyclohexadienones such as **11**.[1–3] In all other cases the incidence of 1,5-cyclisation has needed to be inferred from the presence of rearranged six-membered ring products. We have furthermore used the ratio of directly-cyclised to rearranged six-membered ring products as a basis for estimating cyclisation regioselectivities.

For example, in some cases (R = Me, OMe, Cl),[5,6] the *para*-substituted intermediates **1** and **2** have been found to give two isomeric chromans upon cyclisation (Scheme 1), of which the 7-substituted chroman **9** is formed directly *via* 1,6-cyclisation.

We have proposed that the 6-substituted isomer **10** stems from 1,5-cyclisation, which leads initially to the 8-substituted 1-oxaspiro[4.5]deca-6,9-dien-8-yl radical **3**. Provided oxidation of this radical occurs, the resulting carbocation **6** is suggested to undergo a [1,6]-sigmatropic rearrangement to **8** with migration of carbon being energetically preferred to oxygen. Reactions of this kind are typified in dienone–phenol rearrangements,[7] and we have furthermore demonstrated[3,6] that 1-oxaspiro[4.5]-deca-6,9-dien-8-one **11** is smoothly transformed into 6-hydroxychroman **12** in the presence of acid.

We have no experimental evidence to indicate that the spirocyclohexadienyl radical **3** rearranges similarly.[3] In support of this, we have observed that when the aryl radical cations or alkoxyl radicals are generated using the redox chemistry referred to above, relatively low yields of cyclisation products are obtained unless Cu(II) species are also present. The main function of the Cu(II) is apparently to oxidise the intermediate radicals **3** and **4** to the corresponding carbocations **6** and **7**, and only then do the cyclised products result. Hence in the absence of Cu(II), the spirocyclohexadienyl radical presumably undergoes alternative reactions, probably involving ring-opening.

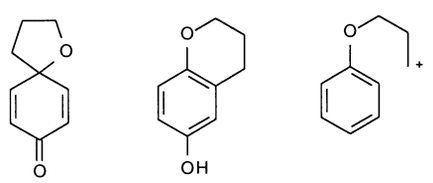

11 **12** **13**

An alternative mechanism for formation of the rearranged chroman involving ring-opening of the spirocyclohexadienyl radical or cation to give an aryloxypropyl radical or the corresponding cation **13** which subsequently undergoes 1,6-ring-closure, can also be discounted since no evidence for the formation of 3-aryloxypropanes or 3-aryloxypropan-1-ols, which would be expected to arise from the ring-opened species under our reaction conditions, has emerged.

Although the rearrangement mechanism which we have proposed to account for the formation of the 6-substituted chromans **10** seems intuitively reasonable, it was considered desirable to quantify the energetics of the process, particularly in view of its importance as the basis for our assessment of the regioselectivity of cyclisation. To this end, we now report on a series of semiempirical and *ab initio* molecular orbital and DFT calculations aimed at investigating the energetics of rearrangement of the parent 1-oxaspiro[4.5]deca-6,9-dien-8-ylium ion **14** to its isomers **16** and **18**. In addition, the characteristics of the transition structures which could be associated with these rearrangement pathways have been explored.

† Electronic supplementary information (ESI) available: the heats of formation and total energies, Mulliken charges, and cartesian coordinates computed for all structures have been tabulated. See http://www.rsc.org/suppdata/p2/b1/b105629h/

 DOI: 10.1039/b105629h

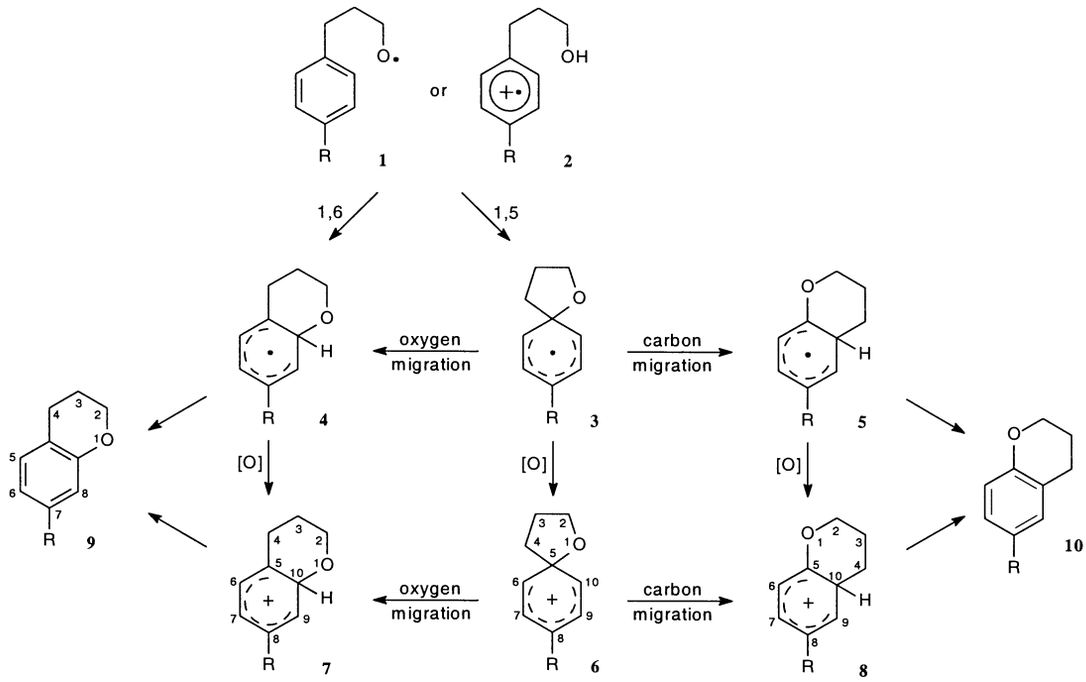

Scheme 1

Results and discussion

The fully-optimised geometries of the 1-oxaspiro[4.5]deca-6,9-dien-8-ylium ion **14**,‡ its two possible rearrangement products **16** and **18**, the associated transition structures **15** and **17** (Scheme 2), and also the 3-phenoxypropylium ion **13** were

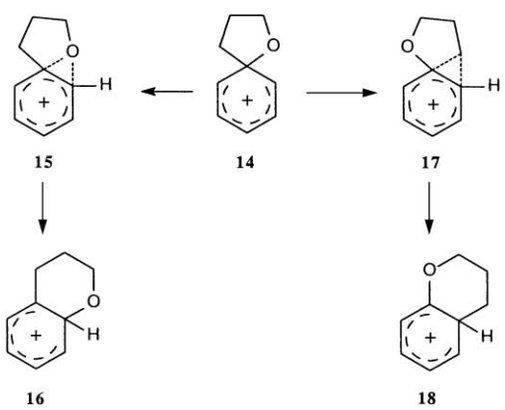

Scheme 2

initially computed at the AM1[8] semiempirical molecular orbital level of approximation.§

Subsequently, the AM1 geometries of **14**, **16** and **18** were refined further at the HF/3-21G *ab initio* level and followed in each case by single-point HF/6-31G*//3-21G calculations. In addition, single-point HF/3-21G//AM1[10] and HF/6-31G*//AM1 calculations were carried out on all of these structures except **13**. Furthermore, the structures **14**–**18** have been refined by optimisation at the B3LYP/6-31G* level of density functional theory followed by single-point energy evaluations at the MP2/6-31G* level for these geometries.[11] The computed AM1 heat of formation and *ab initio* and B3LYP total energies of the structure **14** as well as the relative energies of **15**–**18** are given in Table 1.

Calculated geometries and charge distributions

The AM1 geometry-optimised structure calculated for the spirocyclohexadienyl cation **14** comprises virtually planar five- and six-membered rings linked orthogonally at the spiro junction [Fig. 1(a)]. The C(5)–O bond length is 1.43 Å. Comparison

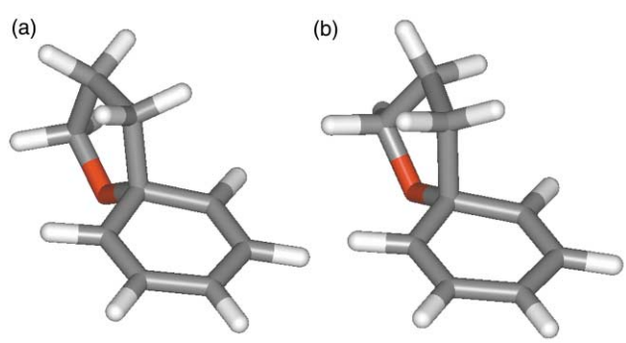

Fig. 1 AM1 and B3LYP/6-31G* optimised structure **14**. (a) AM1, (b) B3LYP/6-31G*.

of the net atomic charges shows that the positive charge resides chiefly on the C(8) centre and, to a lesser extent, also on C(6) and C(10).

In contrast, the HF/3-21G and B3LYP/6-31G* geometry optimisations of **14** give rise to almost identical structures in which the five-membered ring is distinctly puckered, with C(3) being displaced from the plane [Fig. 1(b)]. Also, the HF/3-21G calculation localises marginally less of the positive charge on C(8) than on C(6) and C(10), while an almost uniform distribution of the charge between these three centres is obtained from the B3LYP/6-31G* computation. However, a significantly greater differentiation in the charge distribution between C(6), C(8) and C(10) on one hand and C(7) and C(9) on the other, is again evident in the MP2 single point calculation (Fig. 2).¶

‡ The numbering sequences depicted in structures **6**, **7** and **8** were adopted for the spirocyclohexadienyl cations and their rearranged isomers, while the convention for chromans is shown for **9**.

§ There are numerous examples of semiempirical MO calculations in which the AM1 hamiltonian has been successfully applied to carbocations; see, *e.g.*, ref. 9.

¶ Fig. 2 clearly displays the characteristic alternating charge distributions in the cyclohexadienyl rings of the various carbenium ions.

Table 1 AM1 heat of formation and *ab initio* and density functional total energies of cation **14**, relative energies of cations **15**–**18′**, and theoretical rearrangement rate constants at 298 K

	ΔH_f/kJ mol^{-1}	E_{tot}/hartrees[a]					
	AM1	HF/3-21G//AM1[b]	HF/6-31G*//AM1[b]	HF/3-21G	HF/6-31G*//3-21G[b]	B3LYP/6-31G*	MP2/6-31G*//B3LYP/6-31G*[b]
14	730.1	−419.42963	−421.77752	−419.45115	−421.79323	−424.49222	−423.09888
Relative energies/kJ mol^{-1}							
15	102.7	43.4	59.0			39.3	31.6
16	−46.3	−30.5	−41.2	−15.7	−33.2	−32.8	−22.8
17	74.3	22.6	42.7			15.7	7.6
18	−99.3	−113.4	−112.5	−106.7	−113.3	−119.0	−114.3
18′	−95.2			−105.8		−114.0	−108.0
15–**17**	28.4	20.8	16.3			23.5	24.0
Theoretical rearrangement rate constants/s^{-1}							
k_O[c]/A	9.8×10^{-19}	2.5×10^{-8}	4.5×10^{-11}			1.3×10^{-7}	2.9×10^{-6}
k_C[c]/A	9.4×10^{-14}	1.1×10^{-4}	3.3×10^{-8}			1.7×10^{-3}	4.6×10^{-2}
k_C/k_O	9.5×10^{4}	4.5×10^{3}	7.0×10^{2}			1.3×10^{4}	1.6×10^{4}

[a] 1 hartree = 4.360×10^{-18} J. [b] Single point calculations. [c] Theoretical rate constants for the rearrangement of **14** to **16** and **18**, respectively, calculated from the Arrhenius expression, $k = A \exp(-E_a/RT)$, at 298 K.

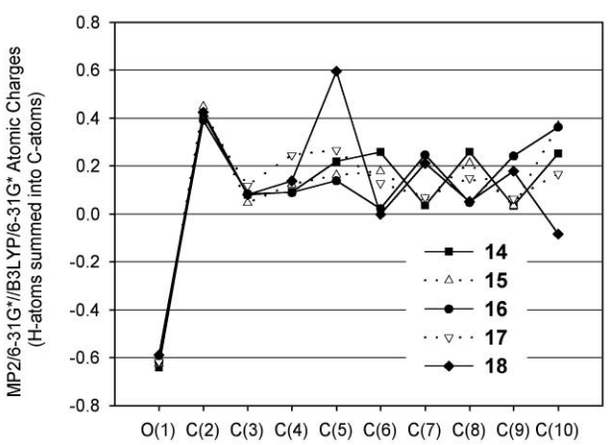

Fig. 2 MP2/6-31G*//B3LYP/6-31G* atomic charges (C-atoms summed with bonded H-atoms) for structures **14**–**18**.

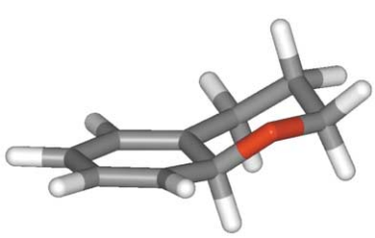

Fig. 3 AM1 optimised structure **16**.

In the AM1-optimised structure of the 1,6-cyclised cation **16** (Fig. 3) the cyclohexadienyl ring is found to be slightly buckled with C(10) being forced downward by the bonded oxygen (C–O bond length 1.42 Å), while the other five carbons remain essentially coplanar, thus ensuring maximal delocalisation of the charge. The fused pyran ring is able to adopt a chair-like conformation. This calculation places the positive charge mainly on the C(7), C(9) and, to a lesser extent, C(5) centres. The geometry of the HF/3-21G optimised structure is similar, as is its charge distribution except that the C(9) centre is slightly more positive than C(7). The B3LYP structure is also similar although the C(10)–O bond is marginally shorter; in this case the charge is fairly evenly distributed over C(5), C(7) and C(9). The MP2 calculation places more significantly more charge on C(7) and C(9) than on C(5) (Fig. 2).

Significantly less distortion of the cyclohexadienyl ring is evident in the rearranged cation **18** [Fig. 4(a)]. The oxygen atom

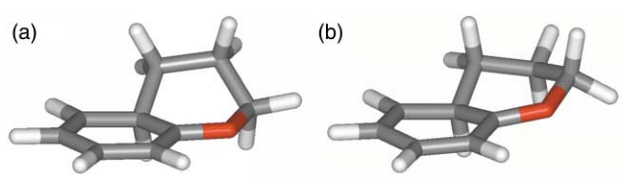

Fig. 4 AM1 optimised structure **18** and **18′**. (a) **18**, (b) **18′**.

and C(2) are also practically coplanar with the cyclohexadienyl system as a result of conjugation, which results in significant shortening of the C(5)–O bond [1.33 Å (AM1), 1.29 Å (3-21G) and 1.30 Å (B3LYP)].‖ The requisite coplanarity of C(10), C(5), O(1) and C(2) is accommodated through the pyran ring adopting a slightly twisted boat conformation. The AM1 positive charge is centered mainly on the C(7) and C(5) centres and, to a lesser extent, C(9) and the oxygen atom. The 3-21G, 6-31G*//3-21G, B3LYP and MP2 calculations concentrate the charge to a significantly greater extent on C(5) and less on oxygen, compared with AM1. Interestingly, in the 3-21G case the oxygen atom is revealed to harbour less positive charge than in either **14** or **16**.

Another slightly less stable conformation **18′** of the cation **18** was also uncovered [Fig. 4(b)]. In this case the pyran ring adopts a distorted chair shape, with a C(10)–C(5)–O(1)–C(2) torsion angle of *ca.* 17°. Twisting of the C(5)–O(1) bond reduces the ability of the oxygen atom to stabilise the positive charge through conjugation and as a result, the electron density on the oxygen atom is marginally higher in **18′** than in **18**. The cyclohexadienyl ring also shows greater distortion from planarity in **18′**. Very similar geometries to the above were obtained for **18′** from both the HF/3-21G and B3LYP optimisations.

Transition structures associated with the two rearrangement routes available to the spirocyclohexadienyl cation **14** were computed at the AM1 semiempirical MO level using MOPAC

‖ By comparison, the computed length (AM1) for the corresponding bond in chroman is 1.38 Å.

methodology, and subsequently by means of the B3LYP/6-31G* method. The resulting structures **15** (Fig. 5) and **17** (Fig. 6) were characterised as first-order saddle points through

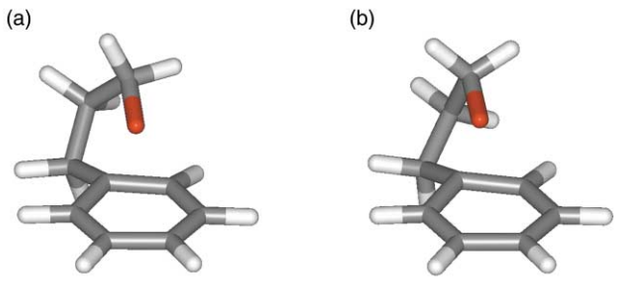

Fig. 5 AM1 and B3LYP/6-31G* optimised structure **15**. (a) AM1, (b) B3LYP/6-31G*.

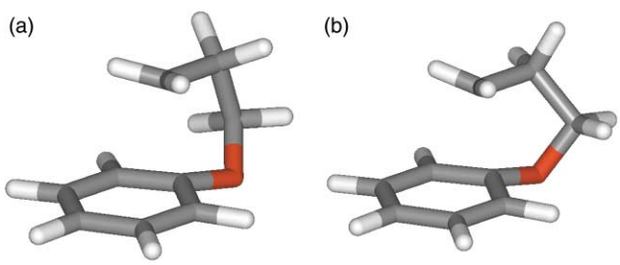

Fig. 6 AM1 and B3LYP/6-31G* optimised structure **17**. (a) AM1, (b) B3LYP/6-31G*.

normal-mode analysis which in each case revealed the presence of a single imaginary vibrational frequency whose eigenvector corresponded to the expected rearrangement. **

In the AM1 transition structure **17** [Fig. 6(a)] resulting from migration of carbon, the migrating carbon C(4) is located 2.17 Å from its origin C(5) and 2.38 Å from its terminus C(10) and is partially flattened. The latter effect is attributed to a significant accumulation of positive charge on this carbon atom and hence a disturbance of its sp^3-hybrid character. †† The geometry of C(5) is already almost planar; the C(5)–O bond is inclined by only about 12° from the general plane of the cyclohexadienyl ring (compared to *ca.* 48° in the spirocyclohexadienyl cation **14**). In contrast, the migration terminus C(10) shows little deviation from planarity. Interestingly, the incipient six-membered ring has already adopted a distorted boat-like shape. It is also noteworthy that the charge distribution within the cyclohexadienyl ring reflects the changes expected during conversion of the spirocyclohexadienyl cation **14** to the isomer **18**, but still resembles the former more closely than the latter.

The B3LYP/6-31G* calculation gives a tighter transition structure **17** [Fig. 6(b)] in which the migrating carbon C(4) is roughly 0.1 Å closer to both C(5) and C(10). Furthermore, the incipient six-membered ring assumes a more favourable chair-like geometry. The charge distribution is similar, except that C(5) is now more positive than the migrating centre C(4). The charge difference between these two centres is smaller in the MP2 calculation while a more distinct alternation between C(6), C(8) and C(10) on one hand, and C(7) and C(9) on the other, is also evident.

In the alternative AM1 transition structure **15** [Fig. 5(a)] which arises from a 1,2-shift by oxygen, the oxygen atom is positioned 1.55 Å from C(5) and 1.69 Å from its destination C(10). The expanding five-membered ring has largely retained its planar geometry, while translocation of the oxygen atom towards C(10) has resulted in the plane of this ring being tilted with respect to that of the cyclohexadienyl ring. In this case too, C(5) is nearing planarity with the C(5)–C(4) bond projecting some 14° below the plane of the cyclohexadienyl ring, compared with *ca.* 60° in the parent system **14**. Some shift of positive charge to the oxygen atom is evident, but is much less pronounced than that experienced by C(4) in the alternative transition structure **17**.

The B3LYP/6-31G* transition structure **15** [Fig. 5(b)] is found to be more reactant-like than its AM1 counterpart with the oxygen atom being located marginally closer to C(5) and *ca.* 0.2 Å further from C(10). Moreover, C(5) also displays more residual pyramidal character.

The charge distributions obtained from single-point calculations in which the 6-31G* polarization basis set was applied to the HF/3-21G and AM1 optimised structures, are similar to those obtained for the 3-21G calculations. However, in all cases the electron densities on the C(2) and C(3) centres are found to be lower. It is also evident that the electron density is increased on O(1) in **15** and on C(5) in **18**. Significantly lower electron densities are indicated for C(5) in both **14** and **15** and for C(10) in **16** and **18**.

Energies

Comparison of the AM1 heats of formation reveals that rearrangement of the spirocyclohexadienyl cation **14** to the isomer **18** is exothermic by 99.3 kJ mol^{-1} with an enthalpy of activation of 74.3 kJ mol^{-1} (Table 1). The alternative isomerisation to **16** is less than half as exothermic at 46.3 kJ mol^{-1} and the enthalpy of activation higher at 102.7 kJ mol^{-1}. By comparison, HF/3-21G//AM1 and HF/6-31G*//AM1 single point as well as the B3LYP/6-31G* calculations indicate that rearrangement of **14** to **18** is more exothermic and conversion to **16** less exothermic than the above, while the enthalpies of activation for the two processes are significantly lower. The energies of the structures **15**–**18** are shown relative to **14** in Fig. 7.

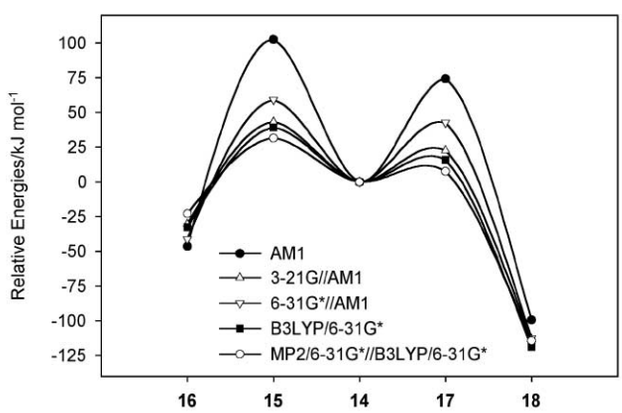

Fig. 7 Energies of structures **15**–**18** relative to **14**.

The HF/3-21G optimisation calculations result in a markedly less exothermic rearrangement of **14** to **16**, while the alternative carbon migration is more exothermic. The results of HF/6-31G*//3-21G single point computations were similar to those obtained for HF/3-21G//AM1.

These findings support our earlier proposal that rearrangement of **14** through migration of carbon is thermodynamically more favourable than migration of oxygen, owing to the superior stabilisation afforded by the conjugated oxygen atom in the cation **18**.

The computed energies of the associated transition structures indicate that migration of carbon is likely to also be the

** The imaginary vibrational frequencies (as wavenumbers/cm^{-1}) for **15** and **17** were 404i and 244i (AM1) and 204i and 223i (B3LYP/6-31G*), respectively.

†† The net atomic charge on C(4) is, however, significantly less positive (0.053) than that calculated for the corresponding atom in the 3-phenoxyprop-3-ylium ion **13** (0.294).

kinetically favoured route. If it is assumed that the entropies of activation associated with the two competing unimolecular rearrangement pathways are similar,‡‡ then the AM1, HF/3-21G//AM1, HF/6-31G*//AM1, B3LYP/6-31G* and MP2/6-31G*//B3LYP/6-31G* activation enthalpy differences are, respectively, 28.4, 20.8, 16.3, 23.5 and 24.0 kJ mol^{-1}, which correspond with rate constant ratios at 298 K of between about 7.4×10^2 and 9.4×10^4 in favour of carbon migration. The B3LYP and MP2 results confirm the essential correctness of the qualitative picture arising from the simpler theoretical methods; further increases in basis-set size or extent of electron correlation are unlikely to affect the result indicating a clear preference for carbon migration.

Conclusion

Our computations have established that rearrangement of the spirocyclohexadienyl cation **14** through a 1,2-shift by carbon is thermodynamically (and probably also kinetically) favoured over the alternative migration by oxygen. Hence, the validity of the mechanism proposed previously to account for the formation of 6-substituted chromans from the alkoxyl radical and aryl radical cation mediated reactions of *para*-substituted 3-phenylpropan-1-ols is confirmed in principle. The effect of ring substituents on the energetics of rearrangement of **14** is currently being investigated and will be reported upon in the near future.

Computational procedure

AM1 calculations were carried out using the MOPAC (version 6.0)§§ software package, and low-level *ab initio* computations using HyperChem (release 4.5),¶¶ both implemented on desktop computers.

AM1 geometries were optimised without constraint using the eigenvector-following routine (keyword EF). Use of the keyword PRECISE ensured that all geometry optimisations achieved energy gradient norms of at least 0.01 kcal mol^{-1} $Å^{-1}$.

AM1 transition structures were determined in MOPAC through application of the SADDLE procedure and optimised using the TS option. Normal-mode analyses of the optimised structures were carried out using the FORCE keyword in order to verify that in each case the Hessian yielded one and only one imaginary frequency. Internal reaction coordinate (IRC) calculations established that both transition structures connected smoothly with the reactant and respective product structures.

Single-point HF/3-21G and HF/6-31G* *ab initio* calculations on selected AM1 and 3-21G geometry-optimised structures were carried out in HyperChem to a SCF convergence limit of 1×10^{-5} kcal mol^{-1}. Convergences were accelerated through application of the DIIS procedure. The HF/3-21G geometry optimisations utilised the Polak–Ribiere optimisation algorithm and were terminated upon achieving energy gradient norms of at least 0.01 kcal mol^{-1} $Å^{-1}$.

Density functional and Møller–Plesset calculations were performed using the Gaussian98 program[11] on a Silicon Graphics Origin 2000 system at the University of Bath. Saddle-point location was initiated from the AM1 geometry and coordinates.

The computed energies of structure **14** and relative energies of **15**–**18′** are reported in Table 1. The AM1 heats of formation and *ab initio* and density functional total energies of all structures are shown in Table S1, the charge distributions in structures **14**–**18** in Table S2, and the atomic coordinates and charges for structures **14**–**18′** in Tables S3–18, all of which have been deposited as supplementary material. The depository also includes the structures in *xyz*-file formats where bonding geometries can be conveniently viewed using visualisation programs such as WebLab ViewerLite.||||

Acknowledgements

CWM acknowledges the National Research Foundation (South Africa) and University of Port Elizabeth for financial assistance, and IHW thanks the HEFCE/EPSRC JREI for computer equipment.

‡‡ The total entropies calculated for the transition structures **15** and **17** at the B3LYP/6-31G* level were 359 J K^{-1} mol^{-1} and 365 J K^{-1} mol^{-1}, respectively; the entropy contributions to the free energies of these structures are estimated to differ by less than 2 kJ mol^{-1} at 298 K.

§§ QCMP 113, Quantum Chemistry Program Exchange, Department of Chemistry, Indiana University, Bloomington, Indiana, 47405, U.S.A.

¶¶ Hypercube, Inc., 1115 N. W. 4th Street, Gainesville, FL 32601, U.S.A.

|||| Freeware available from Molecular Simulations Inc. (http://www.accelrys.com/viewer).

References

1 A. Goosen and C. W. McCleland, *J. Chem. Soc., Chem. Commun.*, 1975, 655.
2 A. Goosen and C. W. McCleland, *J. Chem. Soc., Perkin Trans. 1*, 1978, 646.
3 A. Goosen and C. W. McCleland, *S. Afr. J. Chem.*, 1978, **31**, 67.
4 B. C. Gilbert and C. W. McCleland, *J. Chem. Soc., Perkin Trans. 2*, 1989, 1545.
5 A. Goosen, C. W. McCleland and F. C. Rinaldi, *J. Chem. Soc., Perkin Trans. 2*, 1993, 279.
6 A. Goosen, C. F. Marais, C. W. McCleland and F. C. Rinaldi, *J. Chem. Soc., Perkin Trans. 2*, 1995, 1227.
7 See *e.g.* (*a*) J. March, *Advanced Organic Chemistry: Reactions, Mechanisms and Structure*, 4th edn., Wiley, New York, 1992, p. 1079; (*b*) D. A. Whiting, in *Comprehensive Organic Chemistry*, eds. D. H. R. Barton and W. D. Ollis, Pergamon Press, Oxford, 1979, vol. 1, p. 726; (*c*) R. S. Ward, *Chem. Brit.*, 1973, **9**, 444; (*d*) J. M. Marx and Y.-S. P. Hahn, *J. Org. Chem.*, 1988, **53**, 2866; (*e*) J. N. Marx, J. Zuerker and Y.-S. P. Hahn, *Tetrahedron Lett.*, 1991, **32**, 1921.
8 M. J. S. Dewar, E. G. Zoebisch, E. F. Healy and J. J. P. Stewart, *J. Am. Chem. Soc.*, 1985, **107**, 3902.
9 A. Mahmoud El-Nahas and T. Clark, *J. Org. Chem.*, 1995, **60**, 8023.
10 (*a*) J. S. Binkley, J. A. Pople and W. J. Hehre, *J. Am. Chem. Soc.*, 1980, **102**, 939; (*b*) M. S. Gordon, J. S. Binkley, J. A. Pople, W. J. Pietro and W. J. Hehre, *J. Am. Chem. Soc.*, 1982, **104**, 2797; (*c*) W. J. Pietro, M. M. Francl, D. J. Defrees, J. A. Pople and J. S. Binkley, *J. Am. Chem. Soc.*, 1982, **104**, 5039.
11 Gaussian 98, Revision A. 6 : M. J. Frisch, G. W. Trucks, H. B. Schlegel, G. E. Scuseria, M. A. Robb, J. R. Cheeseman, V. G. Zakrzewski, J. A. Montgomery, R. E. Stratmann, J. C. Burant, S. Dapprich, J. M. Millam, A. D. Daniels, K. N. Kudin, M. C. Strain, O. Farkas, J. Tomasi, V. Barone, M. Cossi, R. Cammi, B. Mennucci, C. Pomelli, C. Adamo, S. Clifford, J. Ochterski, G. A. Petersson, P. Y. Ayala, Q. Cui, K. Morokuma, D. K. Malick, A. D. Rabuck, K. Raghavachari, J. B. Foresman, J. Cioslowski, J. V. Ortiz, B. B. Stefanov, G. Liu, A. Liashenko, P. Piskorz, I. Komaromi, R. Gomperts, R. L. Martin, D. J. Fox, T. Keith, M. A. Al-Laham, C. Y. Peng, A. Nanayakkara, C. Gonzalez, M. Challacombe, P. M. W. Gill, B. Johnson, W. Chen, M. W. Wong, J. L. Andres, C. Gonzalez, M. Head-Gordon, E. S. Replogle and J. A. Pople, Gaussian, Inc., Pittsburgh PA, 1998.